Am J Transl Res 2020;12(6):2652-2663
www.ajtr.org /ISSN:1943-8141/AJTR0107941

Original Article

Allogeneic fibroblast sheets accelerate cutaneous wound healing equivalent to autologous fibroblast sheets in mice

Takashi Nagase[1], Koji Ueno[1], Takahiro Mizoguchi[1], Makoto Samura[1], Takasuke Harada[1], Kotaro Suehiro[1], Bungo Shirasawa[2], Noriyasu Morikage[1], Kimikazu Hamano[1]

[1]*Department of Surgery and Clinical Sciences, Graduate School of Medicine, Yamaguchi University, Ube, Yamaguchi, Japan;* [2]*Department of Medical Education, Yamaguchi University Graduate School of Medicine, Ube, Japan*

Received January 15, 2020; Accepted May 28, 2020; Epub June 15, 2020; Published June 30, 2020

Abstract: Background/Aims: This study sought to confirm the difference of the wound-healing effect, cell survival, and immune response between autologous fibroblast sheets and allogeneic fibroblast sheets. Methods: Regarding wound healing, autologous or allogeneic fibroblast sheets were transplanted onto a mouse cutaneous wound healing model and the wound contraction rate was evaluated. The luciferase-expressing fibroblast sheet was prepared and the survival of the cell sheet was evaluated by IVIS® after autologous or allogeneic transplantation. Histological evaluation was performed at five and 14 days after transplantation. Results: Allogeneic fibroblast-sheet transplantation showed significant wound contraction at the early phase of wound healing, which was equivalent to that seen with the autologous fibroblast sheets. Luminescence of the autologous and allogeneic luciferase-expressing fibroblast sheets peaked on Day 5, and no luminescence was observed on Day 13. In the allogeneic fibroblast-sheet transplant group, a significant accumulation of immune cells was observed in the healed tissue but not in the early stage of wound healing. Conclusion: The allogeneic fibroblast sheets showed comparable rates of cell survival and wound-healing effects to those of the autologous fibroblast sheets, despite the subsequent immunogenic response. This result supports the potential practical clinical application of scaffold-free allogeneic fibroblast sheets based on the paracrine effect.

Keywords: Cell sheet, allogeneic transplantation, fibroblast, IVIS

Introduction

Chronic wounds have been defined as wounds that remain difficult to heal for four weeks up to more than three months [1]. In the United States, chronic wounds affect around 6.5 million patients, with more than US$25 billion each year spent in this area by the health care system [2]. These diseases can lead to a loss of function and decreased quality of life of the patient; moreover, the increasing prevalence rates have become a costly problem in health care [3]. Almost all chronic wounds are categorized as venous ulcers or arterial leg ulcers, diabetic ulcers, or pressure ulcers [4]. Chronic wounds last on average 12 to 13 months, and recurrence rates range from 24% to 57% for venous ulcers, upward of 60% for diabetic ulcers, and 23% to 40% for pressure ulcers [5]. For chronic wounds for which conventional therapy is not effective, advanced therapies such as growth factors, extracellular matrices (ECMs), engineered skin, and negative pressure wound therapy (NPWT) are used. However, decision-making in the selection of these advanced therapies is often not evidence-based [3, 6] and the development of more effective and less expensive treatments is desired.

We previously reported on the therapeutic effects of autologous bone marrow cell implantation during a clinical trial involving eight patients with arterial ulcers who failed conventional revascularization therapy [7]. We also reported that hypoxic preconditioning increases the cell survival and angiogenic potency of bone marrow cells and peripheral blood mononuclear cells [8-10]. On the other hand, cell sheet technology has been established to improve the engraftment of transplanted cells in grafted regions [11] and its therapeutic viability has been demonstrated in various disease models [12-14]. We developed a mixed-cell sheet consisting of autologous peripheral blood mononuclear cells and fibroblasts and reported wound-healing effects in a rabbit lower-limb ischemia model and diabetes mouse model [15, 16]. Furthermore, it was reported that the multilayered sheet shows a higher secretion ability than single-layered sheet [17]. In the prior mouse wound-healing model experiment, the mixed-cell sheet showed more angiogenesis than the fibroblast-only sheet, but the wound-healing effect was equivalent. It is estimated that 45% to 90% of all leg ulceration are of venous origin [18], so the angiogenic potential obtained by mixing peripheral blood mononuclear cells may not be important in the treatment of many chronic wounds. In order to widely spread cell sheets as regenerative medicine products, cells that have a significant range of secretory abilities and that are inexpensive and easy to handle are required. Fibroblasts are critical in all wound-healing phases, including the deposition of ECM components, wound contraction, and remodeling of new ECM. Associated with these various biological roles, fibroblasts produce and respond to a broad array of paracrine and autocrine signals such as cytokines and growth factors [19]. In recent years, while the multifunctional and responsive abilities of mesenchymal stem cells (MSCs) have attracted attention in regenerative medicine, fibroblasts were reported as a practical alternative to MSCs because of their ease in undergoing cell harvesting and high proliferative potential in vitro [20].

In the clinical use of autologous fibroblast sheets, a biopsy from the patient's skin or oral mucosa, prolonged in vitro culture for cell expansion, and quality inspection of regenerative medical products are required for each therapy. The use of autologous cells individually incurs the invasion of the patient, the time required for culture, and the cost of the quality inspection, which limits clinical applications. In contrast, a stock of quality-tested allogeneic cells minimizes those problems and promotes the widespread application and industrialization of regenerative medicine using uniform cells that are not affected by the quality of autologous donor cells. Allogeneic cell-based therapies in wound healing began with products consisting of cultured skin substitute by fibroblasts and keratinocytes and are still being marketed. However, since allogeneic cells do not engraft and the healing mechanism of these products is not well-understood [19]. We also reported that the cell sheets do not engraft permanently as a graft and that the allogeneic fibroblast sheet exhibits a healing effect without showing strong rejection [15]. These findings suggest that the allogeneic fibroblast sheet that does not eventually survive but exerts a therapeutic effect with a paracrine effect for a certain period. However, the exact nature of the engraftment period and the wound-healing effect of the transplanted fibroblast sheet are unclear. This study thus examined the cell survival and efficacy of the allogeneic fibroblast sheet in wound healing in a mouse cutaneous wound healing model.

Materials and methods

Animals

Male C3H/He and male C57BL/6N mice were purchased from Japan SLC, Inc. (Shizuoka, Japan). All animal procedures were approved by the Institutional Animal Care and Use Committee at Yamaguchi University (#31-093) and the experimental methods used were conducted in accordance with the approved guidelines.

Preparation of cell sheets

Fibroblasts were isolated from the tail skin of mice using collagenase (FUJIFILM Wako Pure Chemical Corporation, Osaka, Japan) and cultured in CTSTM AIM V® (Thermo Fisher Scientific, Waltham, MA, USA) and 10% fetal bovine serum (Thermo Fisher Scientific). Primary fibroblast cells were seeded in a 48-well plate (2.5×10^5 cells/cm^2) using 1 mL of medium consisting of CTSTM AIM V® and HFDM-1 (+) (Cell Science & Technology Institute, Sendai, Miyagi, Japan) supplemented with 5% fetal bovine serum and were incubated under normoxic conditions (37°C, 5% CO_2, atmospheric O_2 concentration) for three days.

Histological analysis

For hematoxylin and eosin (H&E) staining and fluorescent immunostaining, isolated cutaneous tissues or fibroblast sheets transferred on ham were fixed in 10% formalin neutral buffer solution and embedded in paraffin. Sections (3 μm in thickness) were cut and mounted on a glass slide, then deparaffinized in xylene and rehydrated in a graded ethanol series. Heat-induced antigen retrieval was performed in Target Retrieval Solution (S1699; DAKO Cytomation A/S, Copenhagen, Denmark) for 30 minutes at 100°C and incubated with blocking buffer (X0909; DAKO) for 20 minutes at room temperature. The following antibodies were used: rabbit anti-vimentin antibody (ab92547; Abcam, Cambridge, UK), mouse anti-actin, α-smooth muscle-Cy3™ antibody (C6198; Sigma Aldrich, St. Louis, MO, USA), rabbit anti-CD3 antibody (ab16669; Abcam), goat anti-rabbit IgG H&L secondary antibody, Alexa Fluor® 488 conjugate (ab150077; Abcam), goat anti-rabbit IgG H&L secondary antibody, DyLight® 550 conjugate (ab96884; Abcam). All histological images were captured by a BZ-X710 microscope (Keyence, Osaka, Japan) and quantified using the BZ-X Analyzer (Keyence).

Cell viability

Primary fibroblast cells at passage 2 were seeded in a 48-well plate (2.5 × 10^5 cells/cm^2) and reacted for one hour at 37°C in a CO_2 incubator with 120 μL of a 1:5 mixture of MTS reagent (CellTiter 96 Aqueous One Solution Cell Proliferation Assay; Promega, Madison, WI, USA) and media. After incubation, 100 μL of supernatant from each well (n = 4) was transferred to a 96-well plate and assayed at 490 nm on a 2030 ARVO X4 microplate reader (PerkinElmer, Boston, MA, USA).

Enzyme-linked immunosorbent assay (ELISA)

Primary fibroblast cells were seeded in a 48-well plate (2.5 × 10^5 cells/cm^2) and were incubated under normoxic conditions (37°C, atmospheric O_2 concentration) for three days, using 1 mL of medium consisting of CTSTM AIM V®, HFDM-1 (+) (Cell Science & Technology Institute) and 5% fetal bovine serum. Supernatants (n = 3) were collected and assayed for transforming growth factor-β1 (TGF-β1), vascular endothelial growth factor (VEGF), and monocyte chemotactic protein-1 (MCP-1) using the Quantikine Immunoassay Kit (R&D Systems, Minneapolis, MN, USA).

Wound healing models and cell sheets transplantation

Male C3H/He mice were anesthetized with 1.5% isoflurane via inhalation and two equal-sized 5-mm full-thickness cutaneous wounds were created on the dorsal skin with a biopsy punch (n = 5, two wounds per mouse). Male C3H/He mouse fibroblast sheets (autologous transplantation) and male C57BL/6N mouse fibroblast sheets (allogeneic transplantation) were transferred onto skin defects, using Seprafilm® (Kaken Pharmaceutical Co., Ltd., Tokyo, Japan) as a carrier. In the control group, only Seprafilm® was transplanted. All ulcers were covered with ADAPTIC (#2012; Acelity, San Antonio, TX, USA) and Derma-aid® (ALCARE, Tokyo, Japan) for the first 24 hours, then with Airwall Fuwari (#MA-E050-FT; Kyowa, Osaka, Japan), and fixed with a Silkytex bandage (#11893; ALCARE). Along with an 8.5-mm diameter measurement, each wound was photographed with a digital camera on Days 0, 3, 5, 7, and 9. Each photograph was normalized with an 8.5-mm diameter measurement and the wound area was measured by manually tracing each wound edge using the ImageJ software (National Institutes of Health, Bethesda, MD, USA). The wound contraction rate could be calculated as [Day X] = 1 - (wound area [Day X]/ wound area [Day 0]).

Transfection of primary fibroblasts

293T cells were incubated in DMEM medium (# 11995-965; Thermo Fisher Scientific) supplemented with 5% fetal bovine serum by 10-cm dish. A total of 1 ml of Opti-MEM™ I Reduced Serum Medium (Thermo Fisher Scientific) was transferred to as 1.5-mL tube, which was added to 6 μg of BLIV 2.0 Reporter: MSCV-Luciferase-EF1α-copGFP-T2A-Puro Lentivector Plasmid (#BLIV713PA-1; System Biosciences, LLC, Palo Alto, CA, USA), 4 μg of pPACKH1 HIV Lentivector Packaging Kit (#LV500A-1; System Biosciences), 30 μL of X-tremeGENE HP DNA Transfection Reagent (#6366244001; Roche Holding AG, Basel, Switzerland) followed by mixing and incubation for 20 minutes. The mixture was applied for 293T cells and then cells were incubated overnight. The medium was replaced with fresh medium and incubated for three days. The medium was transferred to a 15-mL tube followed by centrifugation at 3,000 rpm for five minutes, and the supernatant containing lentiviral particles was passed by a syringe filter(#SLPES2545S;HawachScientific,Tokyo,Japan). Primary fibroblasts isolated from C57BL/6N neonatal mice were incubated for three days in AIM-V medium supplemented with 5% fetal bovine serum containing lentiviral particles and polybrene (8 μg/mL, #H9268; Sigma-Aldrich). Luciferase-positive cells were selected using Puromycin (1 mg/mL, #A1113802; Thermo Fisher Scientific).

Preparation of luciferase-Fb sheets and in vivo imaging system

Luciferase-positive fibroblasts were cultured and seeded as the above-mentioned. The luciferase-expressing fibroblast sheets were transplanted onto male C57BL/6N mice (n = 6, autologous transplantation) and male C3H/He mice (n = 5, allogeneic transplantation) using Seprafilm®. In the control group (n = 3, male C57BL/6N mice and n = 3, male C3H/He mice), only Seprafilm® was transplanted. *In vivo* imaging was performed on Days 2, 5, 9, 13. For each mouse, 200 μL of D-luciferin (120 mg/kg, #XLF-1; Promega) was intra-peritoneally injected five minutes before *in vivo* imaging. A luminescent signal was acquired by IVIS® SpectrumBL (PerkinElmer) with an exposure time of five minutes. ROIs of equal areas were set on the wounds of the joint image, and photons per second were quantified using the Living Image® Software 4.4 (PerkinElmer).

Statistical analysis

Values were expressed as means ± standard deviations. Comparisons between two groups were assessed by two-tailed unpaired t-test. Comparisons of the parameters among three groups were performed using one-way analysis of variance followed by Tukey's multiple comparisons test. A probability value of less than 0.05 was considered to be statistically significant. All statistical analyses were performed using the GraphPad Prism 7 software (GraphPad Software, San Diego, CA, USA).

Results

Production of cell sheets and transplantation model

Fibroblasts were isolated from the tail skin of male C3H/He mice and male C57BL/6N mice. We previously detailed a "multi-layered cell sheet" method for preparing a cell sheet using as many cells (5.0×10^5 cells per well of 24-well plates) as possible to prevent spontaneous detachment from the normal culture plate not using a temperature-responsive culture plate [17]. Cultured primary fibroblasts were seeded in a 48-well plate as multi-layered sheets ($2.5 \times 10^5/cm^2$) and incubated under normoxic conditions for three days. The sheets were gently peeled from the bottom of the culture dish. Male C3H/He mouse fibroblast sheets (autologous transplantation) and male C57BL/6N mouse fibroblast sheets (allogeneic transplantation) were transferred onto skin defects of C3H/He mice to create a 5-mm full-thickness cutaneous wound healing model (**Figure 1A**). By naturally contracting the peeled fibroblast sheet, the diameter of the cell sheet was established at approximately 5 mm (**Figure 1B**) and the thickness of the fibroblast sheet was established at 50 μm (**Figure 1C**).

Equivalence of secretions and viability

To assess growth factors and cytokines secreted from fibroblast sheets, TGF-β1, VEGF, and MCP-1 in the supernatant of each sheet were measured by ELISA. The concentrations of TGF-β1, VEGF, and MCP-1 were the same levels between the supernatant of male C3H/He fibroblast sheets and the male C57BL/6N mouse fibroblast sheets ($P = 0.28$, $P = 0.34$, and $P = 0.81$) (**Figure 2A**). Although TGF-β1 was detected in the culture medium, TGF-β1 in the supernatants of fibroblast sheets was significantly increased relative to in the culture medium (medium vs. C3H/He: $P = 0.0003$, t-test and medium vs. C57BL/6N: $P = 0.0047$, t-test). Both VEGF and MCP-1 remained undetected in the culture medium (data not shown). The cell viability of multilayered fibroblast sheets was measured by MTS proliferation assay. Both fibroblast sheets showed almost the same viability, and the cell viability was increased despite their cell density in vitro (**Figure 2B**).

Evaluation of cell sheet survival by in vivo imaging

To evaluate the cell survival of autologous or allogenic fibroblast sheets, luciferase-expressing fibroblast sheets from C57BL/6N neonatal mice were transferred onto skin defects of C57BL/6N mice (autologous transplantation),

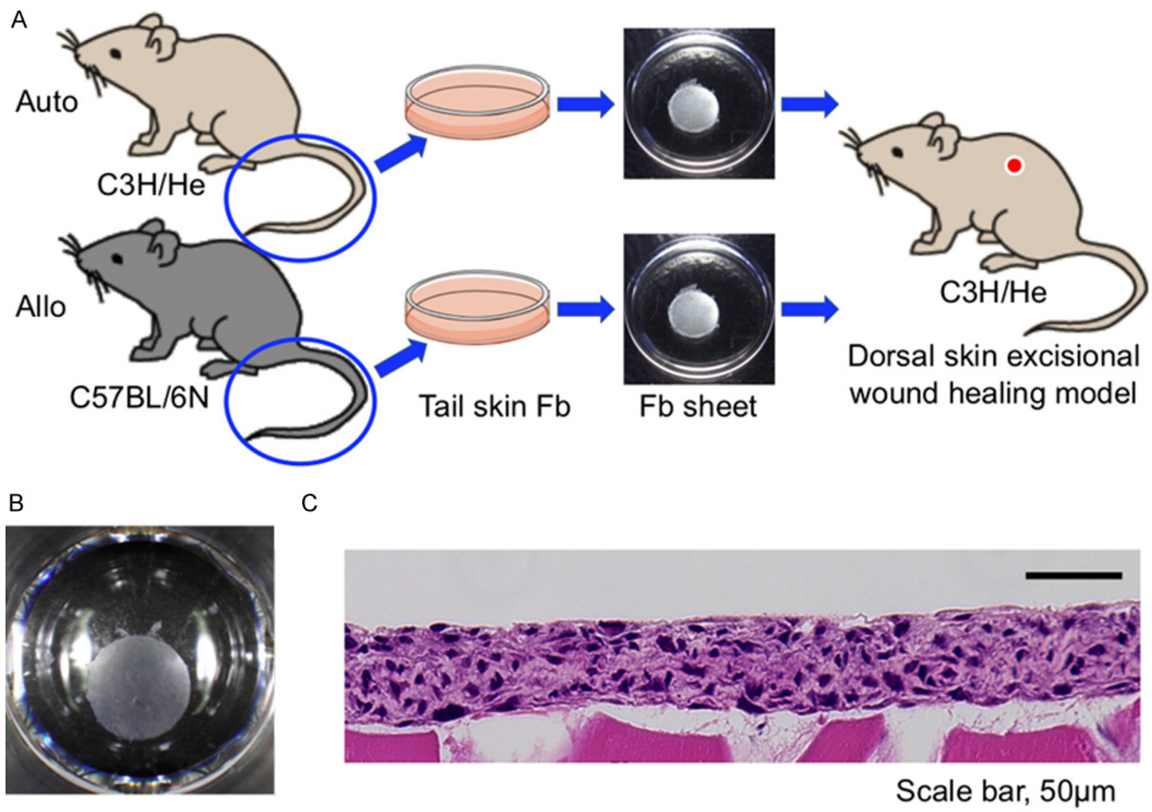

Figure 1. Preparation of fibroblast sheets and transplantation model. A. Fibroblasts were isolated from the tail skin of male C3H/He mice and male C57BL/6N mice. Cultured primary fibroblast cells were seeded in a 48-well plate (2.5×10^5 cells/cm^2) and were incubated under normoxic conditions for three days. The autologous and allogeneic sheets were transferred onto skin defects of C3H/He mouse full-thickness cutaneous wound healing models. B. The macroscopic images of the shape and diameter of one fibroblast sheet peeled from the bottom. The diameter of the well was 10 mm. C. H&E staining shows the thickness of a fibroblast sheet cross-section. Scale bars = 50 μm.

or C3H/He mice (allogeneic transplantation). Representative images demonstrate that all transplanted cells survived to the wound area and were not disseminated beyond the wounds, although they decreased in number over time (**Figure 3A**). Quantified analysis of luminescence signals peaked on Day 5, and the level of luminescence signal was significantly higher in the case of the autologous fibroblast sheet than with the allogeneic fibroblast sheet. On Day 9, there was no statistical difference noted in luminescence signals among the three groups. On Day 13, luminescence signals were not detected (**Figure 3A**, *: $P < 0.01$, **: $P < 0.0001$).

Wound contraction in a mouse cutaneous wound healing model

To evaluate the wound-healing effect of cell sheets, male C3H/He mouse fibroblast sheets (autologous transplantation) and male C57BL/6N mouse fibroblast sheets (allogenic transplantation) were transferred onto skin defects in 5-mm dorsal full-thickness cutaneous wound healing models of male C3H/He mice, followed by the evaluation of each wound on Days 0, 3, 5, 7, and 9 (statistically analyzed as n = 10) (**Figure 4A**). The wound contraction rate was significantly higher in the autologous and allogeneic fibroblast-sheet transplantation groups than in the control group on Day 3 [autologous and allogeneic vs. control: 0.218 ± 0.028 ($P < 0.0001$) and 0.221 ± 0.033 ($P < 0.0001$) vs. -0.059 ± 0.044] and on Day 5 [autologous and allogeneic vs. control: 0.470 ± 0.025 ($P = 0.0006$) and 0.466 ± 0.028 ($P = 0.0009$) vs. 0.278 ± 0.041]. On day 7, the wound contraction rate of the allogeneic fibroblast-sheet group was higher than that in the control group, but not statistically significantly so [autologous and allogeneic vs. control:

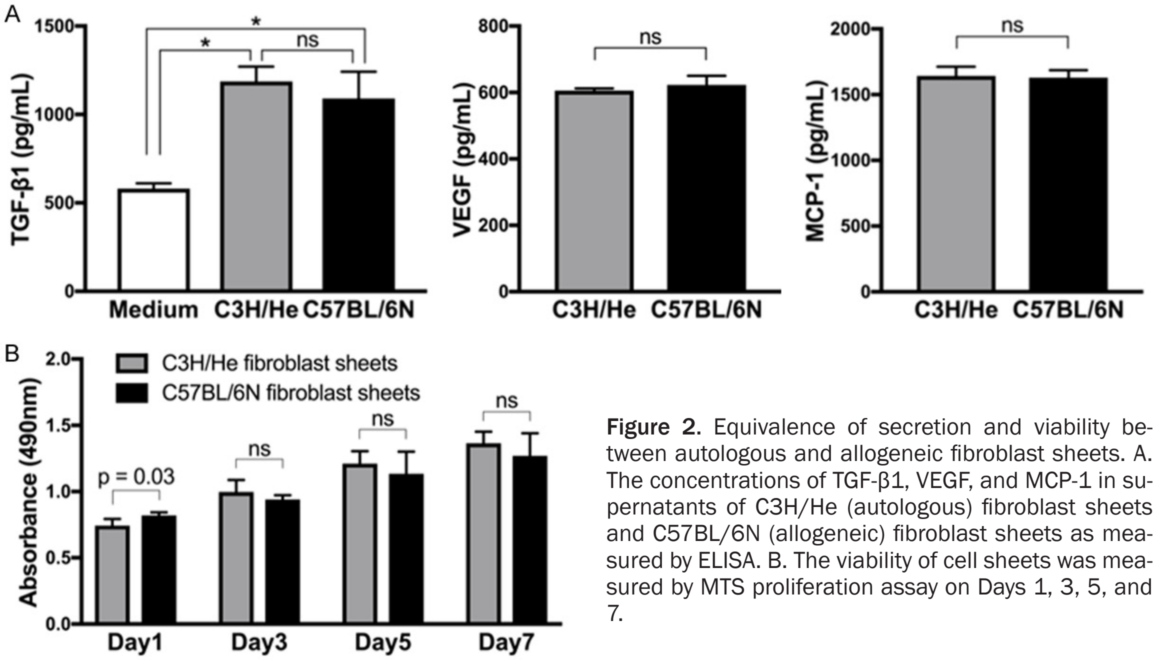

Figure 2. Equivalence of secretion and viability between autologous and allogeneic fibroblast sheets. A. The concentrations of TGF-β1, VEGF, and MCP-1 in supernatants of C3H/He (autologous) fibroblast sheets and C57BL/6N (allogeneic) fibroblast sheets as measured by ELISA. B. The viability of cell sheets was measured by MTS proliferation assay on Days 1, 3, 5, and 7.

0.599 ± 0.024 (P = 0.0094) and 0.569 ± 0.019 (P = 0.077) vs. 0.497 ± 0.024]. There was no significant difference among the three groups (P = 0.11) on Day 9 (**Figure 4B**).

Granulation tissue formation and myofibroblasts of wounds

The appearance of granulation tissue in the bottom of the cut surface, smoothness of the cut edge, and wound contraction were observed in the groups treated with autologous or allogeneic fibroblast sheets by reviewing H&E staining sections on Day 5 (**Figure 5A**). On Day 14, most granulation tissue and wound area were the same in all groups, but more inflammatory cell infiltration was observed in the group of allogeneic fibroblast sheets when compared with the other groups (**Figure 5B**). Immunohistofluorescence staining was performed to clarify the accumulation of myofibroblasts during the wound-healing process. Multicolor staining of vimentin and α-smooth muscle actin (α-SMA) was conducted. Vimentin is a marker of fibroblasts, while the double-positive of vimentin and α-SMA cells shows myofibroblasts. On Day 5, many fibroblasts were observed beside the cut edges of cutaneous ulcers in all groups. More myofibroblasts were observed in groups treated with autologous or allogeneic fibroblast sheets. As compared with on Day 5, a minimal number of myofibroblasts was observed in granulation tissue on Day 14 (**Figure 6A**). The ratio of myofibroblasts to total fibroblasts was significantly higher in the group treated with allogeneic fibroblast sheets than in the control group on Day 5 [allogeneic vs. control: 16.95% ± 1.643% vs. 10.54% ± 1.419%, (P = 0.020)], without a significant difference among the other groups. There was no significant difference among the three groups on Day 14 [control, autologous and allogeneic: 1.888% ± 0.2721%, 1.118% ± 0.2053%, and 1.914% ± 0.4348%, (P = 0.16)] (**Figure 6B**).

Infiltration of T-lymphocytes in the wound-healing process

To investigate the immunological rejection of allogeneic fibroblast sheets onto the wounds, CD3-positive cells as markers of T-lymphocytes were histologically evaluated using immunohistofluorescence. On Day 5, a minimal number of T-lymphocytes infiltrated into the wound among the three groups, whereas, on Day 14, more T-lymphocytes were observed into the wound area in the allogeneic fibroblast sheet treatment group relative to the control and autologous fibroblast-sheet group (**Figure 6C**). The number of T-lymphocytes that infiltrated into the granulation tissues was quantified per area. On Day 5, there was no significant difference among the three groups [control, autologous, and allogeneic: 20.34 ± 23.62 cells/mm^2,

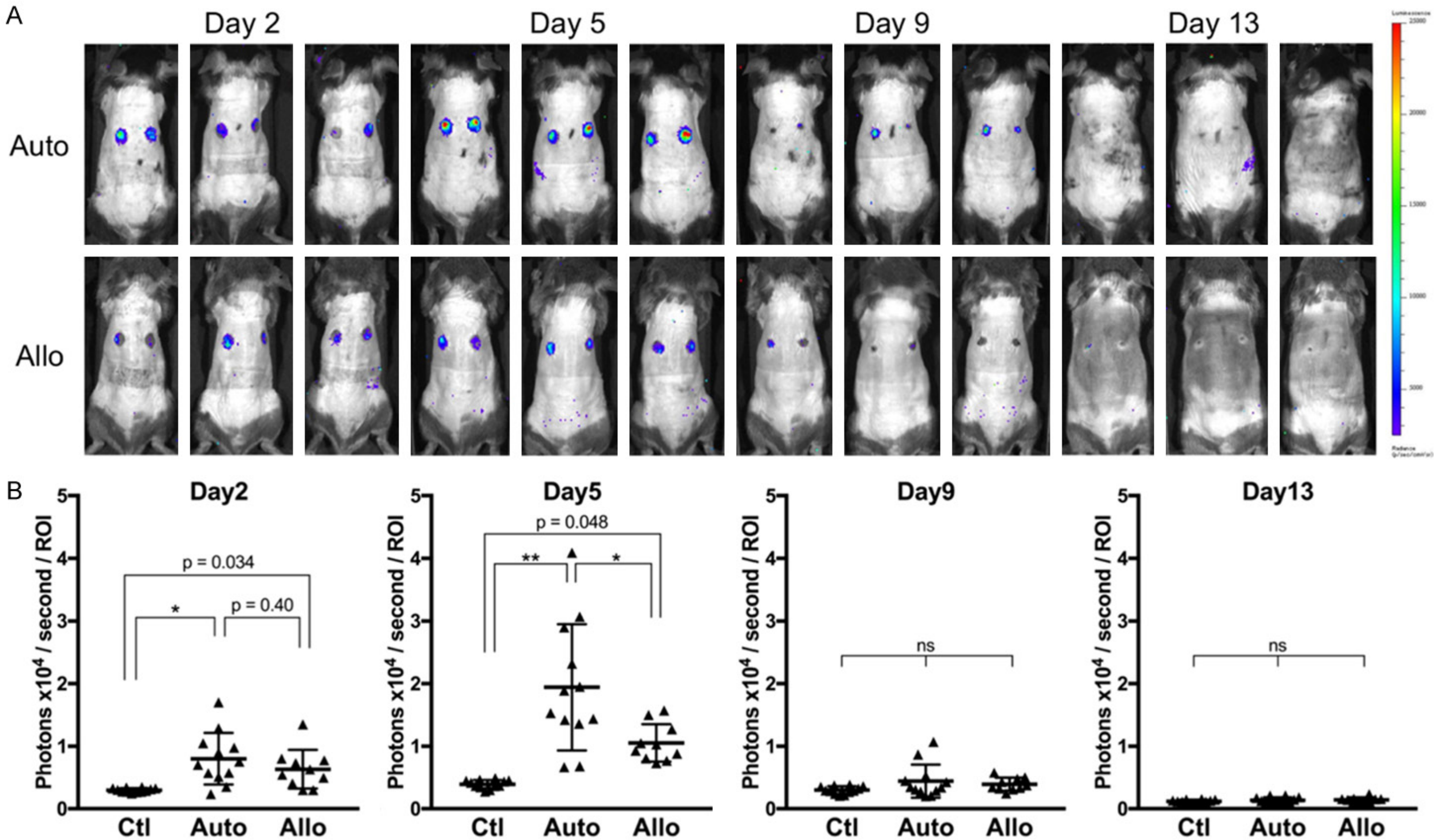

Figure 3. Evaluation of cell sheet survival by an in vivo imaging system. A. Representative fusion images of photo (black and white) and luminescence (color). Luminescent signals by color scale indicate live cells of the transferred luciferase-expressing fibroblast sheets. B. Quantified analysis of luminescence. ROIs of equal area were set on the wounds of the joint image. *: P < 0.01, **: P < 0.0001.

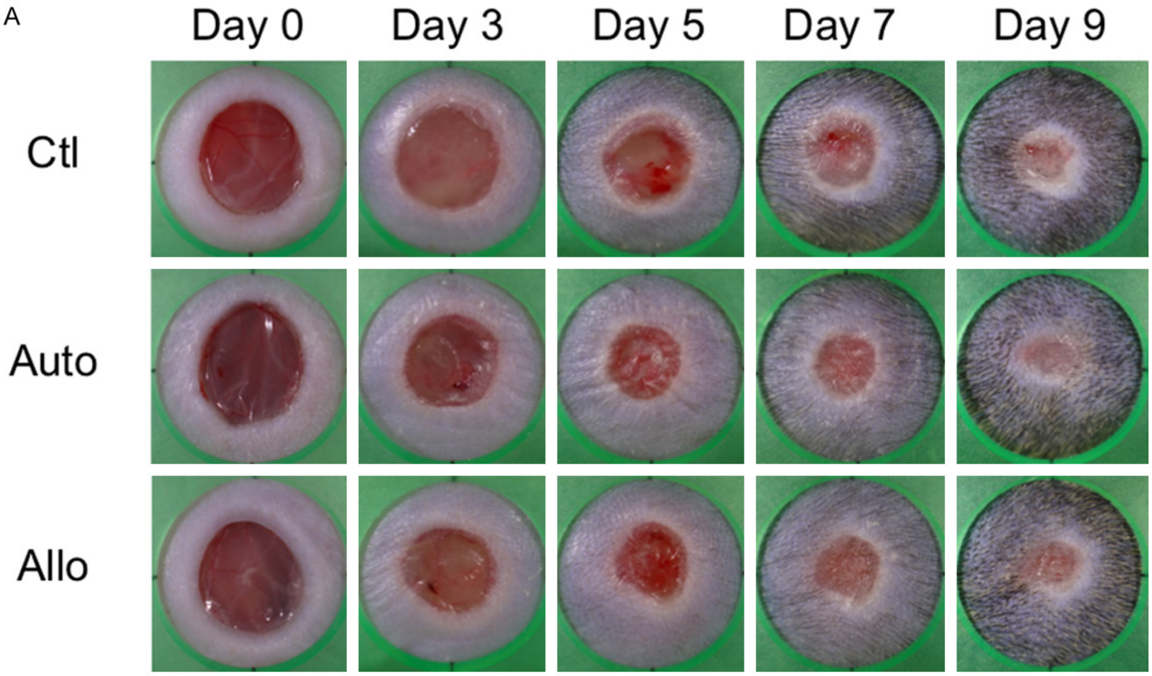

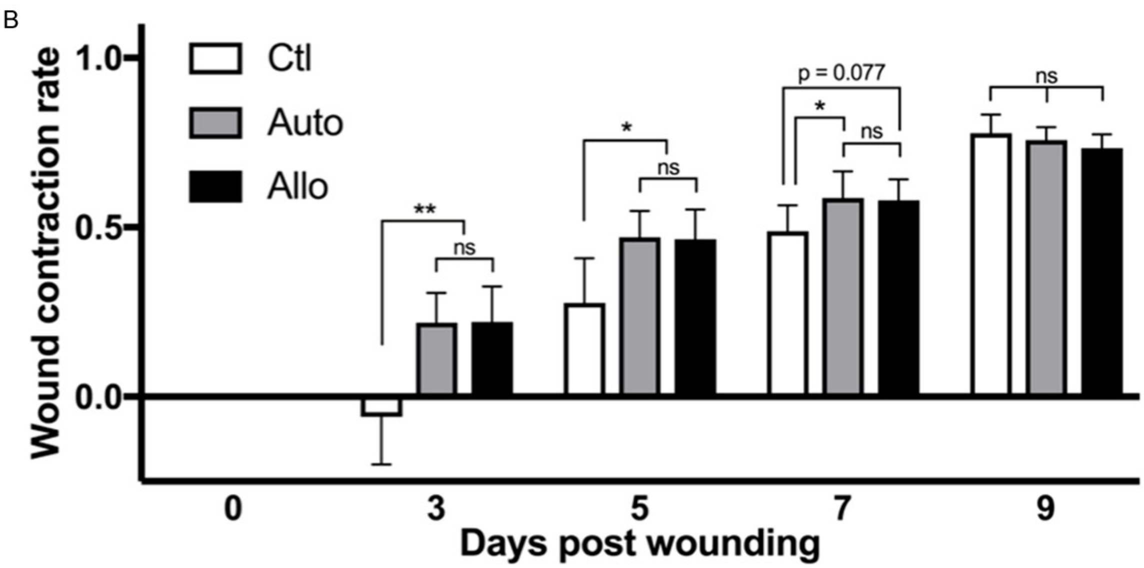

Figure 4. Wound-healing effects of cell sheets on wound contraction. A. Representative macroscopic images of the wound at Days 0, 3, 5, 7, and 9. Male C3H/He mice dorsal full-thickness cutaneous wound healing models, in which wounds received male C3H/He mouse fibroblast sheet transplants (Auto), male C57BL/6N mouse fibroblast sheets (Allo), or carrier-only (Ctl). B. The wound contraction rate after fibroblast transplantation was statistically compared among the three groups by day. *: $P < 0.01$, **: $P < 0.0001$.

18.48 ± 2.676 cells/mm^2, and 20.85 ± 2.471 cells/mm^2, ($P = 0.81$)]. On Day 14, the number of T-lymphocytes of the allogeneic fibroblast-sheet group was significantly higher than that of the control and autologous fibroblast-sheet groups [allogeneic vs. control and autologous: 761.3 ± 87.25 cells/mm^2 vs. 92.88 ± 10.67 cells/mm^2 ($P < 0.0001$) and 87.79 ± 7.074 cells/mm^2 ($P < 0.0001$)] (**Figure 6D**). There was not a significant immunological rejection of allogeneic fibroblast sheets in the early phase of wound healing. A pathological immune response was observed in the tissue after healing on Day 14.

Discussion

Our present data demonstrated that allogeneic fibroblast-sheet transplantation ensures a comparable wound-healing effect to that of

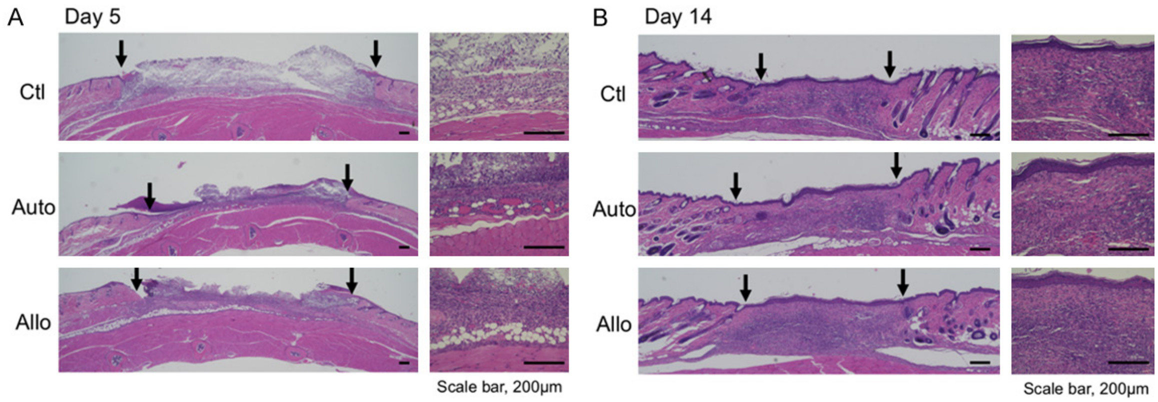

Figure 5. Representative H&E staining section images of the wounds. In the entire images, two arrows indicate both edges of the ulcer. The magnified images show the center of the wounds. A. On Day 5. B. On Day 14. Scale bars = 200 μm.

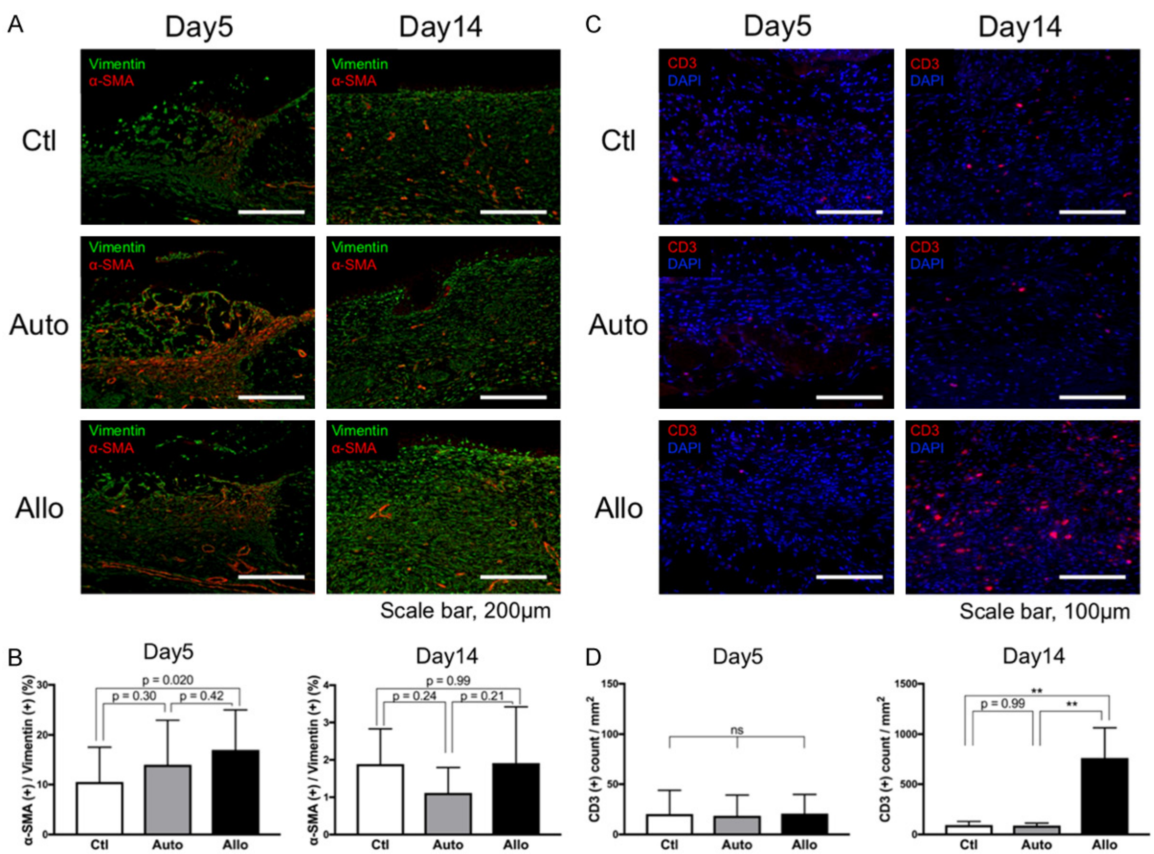

Figure 6. Immunohistochemical fluorescence staining of skin wounds. A. Multicolor staining of vimentin (green) and α-SMA (red). Vimentin-positive cells show fibroblasts. Double-positive cells of vimentin and α-SMA show myofibroblasts at the edges of the ulcer on Day 5 and the center of the wound on Day 14. Scale bars = 200 μm. α-SMA: α-smooth muscle actin. B. Quantified ratio of myofibroblasts to fibroblasts. C. Infiltration into granulation tissues of CD3-positive cells as a marker of T-lymphocytes on Days 5 and 14. T-lymphocyte (CD3: red) and nuclear (DAPI: blue). Scale bars = 100 μm. DAPI: 4',6-diamidino-2-phenylindole. D. Quantified number of CD3-positive cells per mm^2 in granulation tissues on Days 5 and 14.

autologous fibroblast-sheet transplantation, despite histological immune responses. We previously reported that the multilayered sheet (i.e., a scaffold-free, fibroblast sheet with a high cell density) used in this study has the ability to secrete various growth factors and cytokines

[17]. TGF-β1 secreted by the fibroblast sheet promotes ECM production and differentiation of myofibroblasts [21], VEGF promotes angiogenesis, and MCP-1 promotes macrophage chemotaxis, and these all might lead to the wound-healing effect (**Figure 2A**). Both autologous and allogeneic fibroblast sheets showed an equivalent secretion capacity and survival rate (**Figure 2A** and **2B**) and no significant immune cell infiltration was observed in the early phase of wound healing (**Figure 6C** and **6D**). These results might support that a wound-healing effect was occurring to the same degree with both autologous and allogeneic fibroblast sheets (**Figure 4A** and **4B**).

The luminescence of in vivo imaging is proportional to the living number of luciferase-expressing cells. To our knowledge, an analysis by in vivo imaging of the survival of cell sheets in wound healing has not been explored. The analysis of cell sheets by in vivo imaging differs from experiments dealing with the proliferation of tumor cells by in vivo imaging because of measuring the faint emission of decreasing cells in cell sheets. It can be speculated that a temporary increase in the luminescence of the control group during the process of wound healing might constitute background noise due to increased blood flow in conjunction with wound healing, so the amount of luminescence may not accurately reflect the number of living cells in this experiment. However, a significant difference in the amount of luminescence of the luciferase-expressing fibroblast-sheet transplantation group relative to the control group is sufficient to prove the presence or absence of survival of the transplanted cells. In this study, luciferase-expressing autologous or allogeneic fibroblast sheets showed a luminescence peak on Day 5, while no luminescence was observed on Day 13 (**Figure 3A** and **3B**). This result might endorse that the paracrine effect of autologous or allogeneic fibroblast sheets was exhibited early on in transplantation and promoted wound healing at three, five, and seven days after transplantation (**Figure 4**). The cell survival time in allogeneic fibroblast sheets was the same as that in autologous fibroblast sheets. Therefore, allogeneic fibroblast sheets showed the same paracrine effect as autologous fibroblast sheets and disappeared with wound healing, while both autologous and allogeneic fibroblast sheets showed no tumorigenicity.

Fibroblast activation plays a vital role in wound healing; however, in some cases, uncontrolled activation of fibroblasts induces a pathological fibrotic response [19]. Many myofibroblasts were observed in the early phase in wound healing in the fibroblast sheets transplant groups (**Figure 6A** and **6B**), and these myofibroblasts might be induced by TGF-β1 secreted by autologous or allogeneic fibroblast sheets (**Figure 2**) and possibly contributed to wound contraction. However, healed tissue after fibroblast-sheet transplantation did not show an overexpression of myofibroblasts like keloid tissue (**Figure 6A** and **6B**). This suggests that the transplantation of fibroblast sheets is done to promote natural wound healing and might not cause fibrosis and scarring after healing.

Although immunologic problems and the probability of rejection are concerns of allogeneic cell transplantation, clinical signs of rejection such as pain, erythema, and necrosis have not been recognized in regard to the clinical use of cultured skin consisting of allogeneic fibroblasts and keratinocytes [22, 23]. This indicates the safety of the clinical application of allogeneic fibroblasts, but it is unclear as to how their immune response impacts the wound-healing effect. In this study, autologous and allogeneic fibroblast sheets were engrafted in the early phase of transplantation and exerted paracrine effect, so it was though this process the host's immune response to the allogeneic cell sheet began (**Figures 3A**, **3B**, **6C** and **6D**). Because the cell survival of allogeneic cell sheets and autologous fibroblast sheets gradually decreases during wound healing, the reduction of surviving cells in allogeneic fibroblast sheets might keep to the minimum necessary to avoid rejection and, so, rejection might not affect the wound-healing effect.

This study evaluated wound healing in a normal mouse cutaneous wound healing model. Therefore the effect of allogeneic cell sheets in delayed wound healing models may need to be considered. Although the mechanism of wound healing requires further elucidation, our data suggest that the wound-healing effect of allogeneic fibroblast sheets based on the paracrine effect will trigger wound healing for chronic wounds.

In conclusion, the allogeneic fibroblast sheets showed comparable cell survival and wound-healing effects relative to the autologous fibroblast sheets, despite the subsequent immunogenic response. Combined with the high proliferative potential of fibroblasts and the convenience of allogeneic fibroblasts from a cost perspective, scaffold-free fibroblast sheets with a paracrine effect might be a useful future therapeutic agent in clinical practice.

Acknowledgements

We thank Yukari Hironaka for technical assistance. This work was supported by a JSPS Grant-in-Aid for Scientific Research B (15H-04939 to K.H.), and a JSPS Grant-in-Aid for Scientific Research C (18K08735 to B.S.).

Disclosure of conflict of interest

None.

Address correspondence to: Dr. Koji Ueno, Department of Surgery and Clinical Sciences, Yamaguchi University Graduate School of Medicine, Minami-kogushi 1-1-1, Ube, Yamaguchi 755-8505, Japan. Tel: +81-836-22-2261; Fax: +81-836-2423; E-mail: kjueno@yamaguchi-u.ac.jp

References

[1] Jarbrink K, Ni G, Sonnergren H, Schmidtchen A, Pang C, Bajpai R and Car J. Prevalence and incidence of chronic wounds and related complications: a protocol for a systematic review. Syst Rev 2016; 5: 152.
[2] Sen CK, Gordillo GM, Roy S, Kirsner R, Lambert L, Hunt TK, Gottrup F, Gurtner GC and Longaker MT. Human skin wounds: a major and snowballing threat to public health and the economy. Wound Repair Regen 2009; 17: 763-771.
[3] Richmond NA, Maderal AD and Vivas AC. Evidence-based management of common chronic lower extremity ulcers. Dermatol Ther 2013; 26: 187-196.
[4] Nunan R, Harding KG and Martin P. Clinical challenges of chronic wounds: searching for an optimal animal model to recapitulate their complexity. Dis Model Mech 2014; 7: 1205-1213.
[5] Werdin F, Tennenhaus M, Schaller HE and Rennekampff HO. Evidence-based management strategies for treatment of chronic wounds. Eplasty 2009; 9: e19.
[6] Frykberg RG and Banks J. Challenges in the treatment of chronic wounds. Adv Wound Care (New Rochelle) 2015; 4: 560-582.
[7] Li TS, Hamano K, Suzuki K, Ito H, Zempo N and Matsuzaki M. Improved angiogenic potency by implantation of ex vivo hypoxia prestimulated bone marrow cells in rats. Am J Physiol Heart Circ Physiol 2002; 283: H468-473.
[8] Kubo M, Li TS, Kurazumi H, Takemoto Y, Ohshima M, Murata T, Katsura S, Morikage N, Furutani A and Hamano K. Hypoxic preconditioning enhances angiogenic potential of bone marrow cells with aging-related functional impairment. Circ J 2012; 76: 986-994.
[9] Kubo M, Li TS, Suzuki R, Shirasawa B, Morikage N, Ohshima M, Qin SL and Hamano K. Hypoxic preconditioning increases survival and angiogenic potency of peripheral blood mononuclear cells via oxidative stress resistance. Am J Physiol Heart Circ Physiol 2008; 294: H590-595.
[10] Kudo T, Hosoyama T, Samura M, Katsura S, Nishimoto A, Kugimiya N, Fujii Y, Li TS and Hamano K. Hypoxic preconditioning reinforces cellular functions of autologous peripheral blood-derived cells in rabbit hindlimb ischemia model. Biochem Biophys Res Commun 2014; 444: 370-375.
[11] Shimizu T, Yamato M, Kikuchi A and Okano T. Cell sheet engineering for myocardial tissue reconstruction. Biomaterials 2003; 24: 2309-2316.
[12] Matsuura K, Utoh R, Nagase K and Okano T. Cell sheet approach for tissue engineering and regenerative medicine. J Control Release 2014; 190: 228-239.
[13] Sawa Y and Miyagawa S. Cell sheet technology for heart failure. Curr Pharm Biotechnol 2013; 14: 61-66.
[14] Ohki T, Yamato M, Ota M, Takagi R, Murakami D, Kondo M, Sasaki R, Namiki H, Okano T and Yamamoto M. Prevention of esophageal stricture after endoscopic submucosal dissection using tissue-engineered cell sheets. Gastroenterology 2012; 143: 582-588. e582.
[15] Ueno K, Takeuchi Y, Samura M, Tanaka Y, Nakamura T, Nishimoto A, Murata T, Hosoyama T and Hamano K. Treatment of refractory cutaneous ulcers with mixed sheets consisting of peripheral blood mononuclear cells and fibroblasts. Sci Rep 2016; 6: 28538.
[16] Takeuchi Y, Ueno K, Mizoguchi T, Samura M, Harada T, Oga A, Murata T, Hosoyama T, Morikage N and Hamano K. Ulcer healing effect of autologous mixed sheets consisting of fibroblasts and peripheral blood mononuclear cells in rabbit ischemic hind limb. Am J Transl Res 2017; 9: 2340-2351.
[17] Mizoguchi T, Ueno K, Takeuchi Y, Samura M, Suzuki R, Murata T, Hosoyama T, Morikage N and Hamano K. Treatment of cutaneous ulcers with multilayered mixed sheets of autologous

fibroblasts and peripheral blood mononuclear cells. Cell Physiol Biochem 2018; 47: 201-211.
[18] Hedayati N, Carson JG, Chi YW and Link D. Management of mixed arterial venous lower extremity ulceration: a review. Vasc Med 2015; 20: 479-486.
[19] Kendall RT and Feghali-Bostwick CA. Fibroblasts in fibrosis: novel roles and mediators. Front Pharmacol 2014; 5: 123.
[20] Ichim TE, O'Heeron P and Kesari S. Fibroblasts as a practical alternative to mesenchymal stem cells. J Transl Med 2018; 16: 212.
[21] Janson DG, Saintigny G, van Adrichem A, Mahe C and El Ghalbzouri A. Different gene expression patterns in human papillary and reticular fibroblasts. J Invest Dermatol 2012; 132: 2565-2572.
[22] Falanga V, Margolis D, Alvarez O, Auletta M, Maggiacomo F, Altman M, Jensen J, Sabolinski M and Hardin-Young J. Rapid healing of venous ulcers and lack of clinical rejection with an allogeneic cultured human skin equivalent. human skin equivalent investigators group. Arch Dermatol 1998; 134: 293-300.
[23] Donohue KG, Carson P, Iriondo M, Zhou L, Saap L, Gibson K and Falanga V. Safety and efficacy of a bilayered skin construct in full-thickness surgical wounds. J Dermatol 2005; 32: 626-631.